

STATIC AND DYNAMIC STABILITY IN TRANSONIC FLOW

Experimental Determination of the Dynamic Derivatives of a Reentry Capsule in Transonic Supersonic Regime

Sébastien Paris

Aeronautics and Aerospace Department, von Karman Institute for Fluid Dynamics, Belgium, paris@vki.ac.be

Patrick Rambaud

Associate professor, Aeronautics and Aerospace Department, von Karman Institute for Fluid Dynamics, Belgium, rambaud@vki.ac.be

University Supervisor: Gérard Degrez

Professor, Université libre de Bruxelles, Belgium, gdegrez@ulb.ac.be

Abstract

Aerodynamic damping is investigated in the subsonic and transonic regimes for re-entry vehicles. Static moment, free oscillations and forced oscillations experiments are carried out on replica models in the von Karman Institute (VKI) S-1 supersonic-subsonic wind tunnel. The frequency of oscillations induced in wind tunnel is made to match the reduced frequencies of flight vehicles based on their natural frequencies. In free oscillation mode, the inertia of the vehicle is adjusted for the same reason. Recent results on this vehicle with a sting as support are compared with existing data in literature and with a previous campaign carried out in the VKI-S1 with a transversal support on a different experimental set-up. It shows significant effects of the support on the static and dynamic measurement. Proper validation of the methods should give better confidence into the results for the dynamic characterization of the vehicles.

Nomenclature

Symbols

α	Angle of attack, rad
θ	Pitch angle, rad
C_D	Drag coefficient, -
C_L	Lift coefficient, -
C_m	Pitching moment coefficient, -
$C_{m_q} + C_{m_{\dot{\alpha}}}$	Pitching moment derivatives, rad^{-1}
q_∞	Dynamic pressure, Pa
ρ_∞	flow density, kg/m^3
St	Strouhal number, -

Abbreviations

CG	Center of Gravity
CTV	Crew Transport Vehicle
SLA	Stereolithography

1. Introduction

Entry capsules provide an attractive option for planetary exploration missions. Designed to survive during early phases of atmospheric entry, these vehicles often become dynamically unstable at low altitudes. Proper characterization of aerodynamic damping can allow drogue chute deployment at lower Mach number. Such findings may permit smaller drogue chute designs, thus enabling a payload volume and weight increase as well as a vast decrease in drag penalties.

The aerospace vehicle is exposed to unsteady flow fields that may have significant effects on its characteristics of motion. As a result, the dynamic stability information, considered of rather lesser importance for a number of years, has become an object of relatively high interest. The reason is obvious: in the past, for aircrafts at low angles of attack, most of the dynamic stability parameters were relatively easy to predict analytically. It had only a relatively insignificant or at least, a relatively constant effect on the resulting flight characteristics of the vehicle. With the

advent of flight at high angles of attack at high speeds, all that has drastically changed. The dynamic stability parameters are now found to depend strongly on the non-linear effects and can no longer be calculated using relatively simple linear analytical methods as in the past and new methods are needed. Since the non-linear instability phenomena are not well known for the moment, it is in general difficult to simulate them using CFD. Thus, the experimental techniques in wind tunnels are certainly the best way to obtain dynamic stability information at realistic Reynolds and Mach numbers.

2. Objective

The objective of this project is to develop the experimental tools for the study of the dynamic stability in the subsonic and supersonic range. The wind tunnel S1 was selected for this purpose. Different experimental techniques need to be implemented in it. The free oscillation technique consists in releasing the model in a given position and observing the model oscillating around its axis. It gives directly the behavior of the model. The forced oscillation technique does not give directly the characteristic of the model. Oscillations are forced by a crankshaft mechanism and the pitching moment is measured during the oscillations thanks to a balance. These techniques have been developed and used with various reentry vehicle and need to be properly validated in order to assess the uncertainty of the methods.

3. Theory

3.1. Motion equations

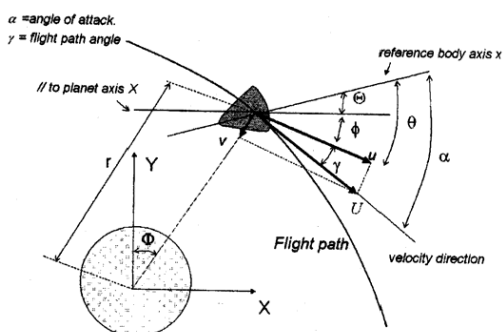


Figure 1: Space vehicle entering the atmosphere [2]

The motion of a space capsule during planetary reentry can be seen, by classical mechanics, as a combination of translation and rotation around its center of

gravity. The classical equations of motion of the vehicle are obtained using a fixed system of coordinates, and assuming the vehicle to be rigid. Then one can deduce the six equations governing the movement of the object in the three dimensions. However since the system obtained is quite complex to solve (impossible analytically), one usually makes some assumptions: the displacement is made in two dimensions, the rotation of the earth is neglected and the gravity force is constant.

In the wind tunnel, the angle of attack and the pitch angle are equals:

$$\theta = \alpha \Leftrightarrow \gamma = 0 \quad (1)$$

A set of three equations governing the movement of the vehicle in two dimensions can be obtained:

$$m \frac{dU_x}{dt} = q_\infty S C_D \quad (2)$$

$$m \frac{dU_z}{dt} = q_\infty S C_L - mg + m \frac{U^2}{r} \quad (3)$$

$$I \ddot{\theta} = q_\infty S C_m D \quad (4)$$

This third equation represents the rotation of the capsule around his pitch axis. The pitching moment coefficient can be rewritten depending on the other parameters:

$$C_m = \frac{\partial C_m}{\partial \alpha} (\alpha - \alpha_0) + C_{m_q} \frac{D}{2U} \dot{\theta} + C_{m_{\dot{\alpha}}} \frac{D}{2U} \dot{\alpha} \quad (5)$$

C_m may be separated into two parts (recalling that α and θ are equivalent here):

- a static one: $\frac{\partial C_m}{\partial \alpha} (\theta - \theta_0)$
- and a dynamic one: $(C_{m_q} + C_{m_{\dot{\alpha}}}) \frac{D}{2U} \dot{\theta}$

Hence the equation 4 can be written:

$$I \ddot{\theta} = q_\infty S C_{m_\alpha} D (\theta - \theta_0) + q_\infty S \frac{D^2}{2U} (C_{m_q} + C_{m_{\dot{\alpha}}}) \dot{\theta} \quad (6)$$

This equation describes the motion of the model around its pitching axis. The C_{m_α} coefficient is the static coefficient which can be known thanks to the static measurement of the pitching moment.

The aim of the present activities is to determinate the dynamic coefficient: $C_{m_q} + C_{m_{\dot{\alpha}}}$.

3.2. Similarity parameters

The experiment conditions are based on the similarity with flight data. The similarity can be made on several parameters, but it is usually impossible to make all of them respected in the same time. As a consequence, one has to choose which ones are of primary importance. Geometry of the model is of course one of them and means that the model should be a scaled representation of the vehicle outer shape. In order to reproduce correctly the movement, the CG location of the flight vehicle should correspond to the center of rotation of the wind tunnel model. Another important parameter to match while performing experiments in transonic and supersonic regime is the Mach number. Here, the experiments deal only with Mach numbers high enough not to neglect the compressible effects, and hence the Mach number similarity has to be applied. Finally, the third parameter to match for the similarity concern is the oscillations reduced frequency. This non-dimensional number is very similar to a Strouhal number, but is based on the frequency of the model oscillations and not on a frequency relating to the flow. It is assumed that this parameter should be matched in order to obtain the same aerodynamic behavior as in flight. The reduced frequency matching depends on the test technique that is used and its computation is presented below. It is worth to mention that the Reynolds number similarity, which is very often a major concern in fluid dynamics experiments, cannot be fulfilled in the classical facilities: it is in fact much lower for the experiments than for the flight due to the large scaling factor, while the other parameters do not changed a lot. However, it is usually admitted that the stability phenomena are affected by the flow regime (meaning laminar or turbulent), and not much by the exact matching of the Reynolds number. For the similarity of this study, the flow in flight is certainly fully laminar and as the Reynolds number reached during experiments is much lower than the one of flight, one can assume that the flow is completely laminar for experiments as well as for the flight.

3.3. Reduced Frequency (Strouhal Number)

The reduced frequencies of both the model and the flight vehicle for the forced oscillation tests should be maintained to equate the dissipation or input of energy from the surrounding flow field (aerodynamic influences) on the model during testing with the flight vehicle. It is defined by the Strouhal number (St). Oscillations occur at the natural frequencies of the actual flight vehicle upon atmospheric re-entry condition. Thus, during free and forced oscillations tests

on the models, the Strouhal number based on the natural frequency and characteristic length of the flight vehicle is used. The general formulation is given by:

$$St = \frac{fD}{U_\infty} \quad (7)$$

Extraction of the natural frequency f of the flight vehicle is obtained from the 'spring' and 'damping' constant in equation 6.

$$f_{flight} = \frac{1}{2\pi} \sqrt{\underbrace{\frac{q_\infty S D |(\partial C_m / \partial \theta)|}{I}}_{\text{static restoring moment}} - \underbrace{\frac{q_\infty S D (C_{m_q} + C_{m_i})}{2I}}_{\text{aerodynamic damping}}} \quad (8)$$

The aerodynamic damping can be neglected due to its magnitude relative to the static restoring moment contribution. Thus, the Strouhal number of the flight vehicle becomes:

$$\begin{aligned} (St)_{flight} &= \left(\frac{fD}{U_\infty} \right)_{flight} \\ &= \left(\sqrt{\frac{\rho_\infty S D^3 |(\partial C_m / \partial \theta)|}{8\pi^2 I}} \right)_{flight} \quad (9) \end{aligned}$$

ρ_∞ is the free stream density. The respect of the similarity provides the value of the inertia and of the driving frequency respectively for the free and forced oscillations:

$$I_{experiment} = \left(\frac{I}{\rho_\infty D^5} \right)_{flight} \times (\rho_\infty D^5)_{experiment} \quad (10)$$

$$f_{experiment} = \frac{1}{2\pi} \left(\sqrt{\frac{\rho_\infty S D^3 \left(-\frac{\partial C_m}{\partial \alpha}\right)}{2I}} \right)_{flight} \times \left(\frac{U_\infty}{D} \right)_{experiment} \quad (11)$$

4. The free oscillations technique

For this technique, the model is free to rotate around an axis passing by the CG location. It is release in a position different of the trim angle. The model is then free to oscillate around the trim angle. The incidence angle is recorded over time. In order

to simplify the writing of the equation of motion, it is replaced by a more general form:

$$\ddot{\theta}(t) + a\dot{\theta}(t) + b\theta(t) = 0 \quad (12)$$

where a and b are two coefficients

One can obtain the damping in pitch parameter from the resolution of this equation with:

$$C_{mq} + C_{m\dot{\alpha}} = -\frac{I\alpha}{q_{\infty}S D \frac{D}{2U_{\infty}}} \quad (13)$$

4.1. Envelope Method

The method used for the resolution of the differential equation and the extraction of the damping in pitch parameter is the envelope method. It consists in using only the maximum or the minimum value of the signal for each oscillation, and in computing the logarithmic decrement between two extrema. For a theoretical second order signal, the oscillations damping is computed by:

$$a = \frac{2}{nT} \ln\left(\frac{x_2}{x_1}\right) \quad (14)$$

T is the period of the signal x_1 and x_2 are two extreme values separated by n periods.

In computing the damping over the whole signal (either by using the first and the last extremum or by making an envelope fitting of the whole signal), a single value is found for the damping in pitch parameter. However, due to the large variation of the oscillations amplitude during the tests, it appeared that this method is too global and does not take into account the possible changes in the damping term: it is not satisfactory.

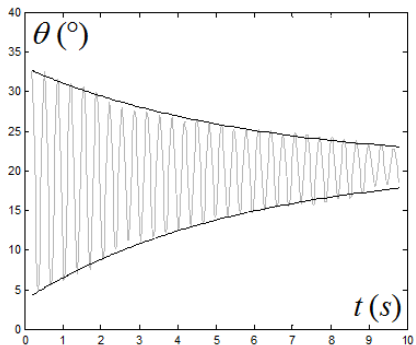


Figure 2: Envelope curves

On the opposite, by calculating the damping value between each two consecutive maxima or minima, the

experimental uncertainty has a large influence on the results, which are therefore very scattered and not usable properly. As a consequence, what it seems to be the best technique is a compromise between the two: the use of about seven oscillations of the signal to perform the average damping over them gives results of a quite accuracy and without a large scattering.

5. The forced oscillations technique

Models oscillate with one degree of freedom over a fixed range of oscillation angles in a periodic pattern. The forced oscillations induce moments on the model in addition to the aerodynamic loads. Moments and incidence angles are recorded over time. Contrary to the free oscillations equation of motion, the equation for forced oscillations cannot be solved directly for the damping in pitch parameter because of the mechanical moments, which cannot be evaluated independently from the actual experiments. However, in performing the so-called no flow measurements (which consist in forcing the oscillations of the model, with the wind tunnel not working), one gets the following equation of motion (like the equation 5 without the aerodynamic terms):

$$I\ddot{\theta}(t) - c\dot{\theta}(t) - k\theta(t) = M_{nf}(t) \quad (15)$$

$M_{nf}(t)$ is the external forcing moment as a function of time in no flow conditions. Then, in computing the difference between the equation 15 with flow and without flow, one finds:

$$q_{\infty}S D \frac{D}{2U_{\infty}} (C_{mq} + C_{m\dot{\alpha}}) \dot{\theta}(t) + q_{\infty}S D C_{m\alpha} \theta(t) = M_{nf}(t) - M_f(t) \quad (16)$$

$M_f(t)$ is the external forcing moment as a function of time in flow conditions. In a more general form, it gives:

$$A\dot{\theta}(t) + B\theta(t) = \frac{\Delta M(t)}{qSD} \quad (17)$$

The mechanical moments as well as the inertial part of the original equation of motion do not appear anymore for the resolution of the problem. However, the use of the two sets (with and without flow) of experiments requires absolutely the equality in the evolution of the angle of attack ($\theta_f(t) = \theta_{nf}(t)$ at every instant). One can obtain the damping in pitch parameter from the resolution of this equation with:

$$C_{mq} + C_{m\dot{\alpha}} = A \frac{2U}{D} \quad (18)$$

The principle of the energy resolution consists in integrating the work absorbed by the system (corresponding to amplification) or dissipated (corresponding to damping) during one oscillation cycle. In fact, since the mechanical friction is not null in the driving system, some energy injection is always necessary to compensate the losses. The energy is injected by the power supply. Depending on the loop direction (see figure 3), one can deduce if the system oscillations would be amplified or damped while subjected to free oscillations. The first case is represented by a counter clockwise loop associated to a dissipation of energy, whereas the second situation is associated to a clockwise loop associated to an input of energy.

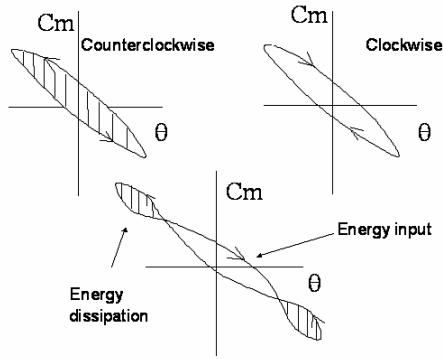


Figure 3: Energy method representation

The general expression of the damping in pitch parameter is the following [2]:

$$C_{m\dot{\alpha}} + C_{mq} = \frac{\oint C_m d\theta}{\int \dot{\theta}^2 dt} \frac{2U}{D} \quad (19)$$

One can notice that, as the graphical representation has shown it, the damping in pitch parameter (about which it has been said that a negative value means dynamic stability) and the pitching coefficient integral are of the same sign.

6. Equipment

6.1. Supersonic / Transonic S-1 Wind Tunnel

The VKI supersonic/transonic wind tunnel S-1 is a continuous closed circuit facility of the Ackeret type, driven by a 615 kW axial flow compressor. Two 40

cm x 36 cm test sections are used: a contoured nozzle with $M = 2.0$ and a slotted transonic section with variable Mach number, from 0.4 to 1.05. The tunnel is equipped with scani-valves for pressure distribution measurements, multi-component strain gage balances, and a free-to-tumble mounting system for investigations of dynamic stability of aerospace vehicles.

Mach	P_0 Pa	p_∞ Pa	$Re_{L_{ref}}$ -	T_0 °C	ρ_∞ kg.m ⁻³	U_∞ m.s ⁻¹
0.5	26685	22514	169306	26	0.2755	168.72
0.6	26681	20891	198116	32	0.2558	203.42
0.69	26772	19421	223702	40	0.2374	234.54
0.8	26695	17565	247673	48	0.2151	269.50
0.89	27710	16248	262591	56	0.2000	299.32
2.0	9430	1193	875900	25	0.0249	519.25

Table 1: Typical Flow conditions

6.2. Experimental setup

Several experimental setups have been designed and build over the years for the static and for the dynamic measurement.

6.2.1. Static experiments

First configuration

The first experimental setup was built during the CTV phase A and one of the purposes was to cover the full domain of interest for the AEDB (360°). The figure 4 shows the next setup where a stepping motor was added in order to rotate the model during the test. The reference length is 50mm, the diameter of the capsule. Static force and moment measurements are now possible in a range of [-225;+225°]. Axial and normal forces are measured by two strain gage balances implemented in the arms. The stepping motor and the angle measurement digital device are mounted on this balance so that all aerodynamic efforts are applied on the balances.

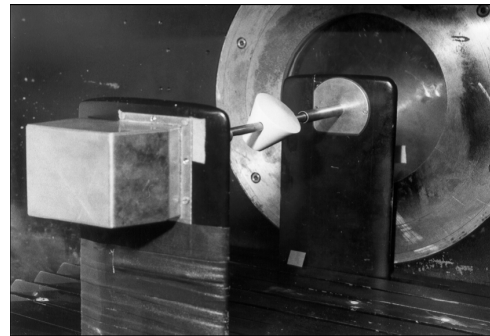


Figure 4: Experimental setup for the static test(improved)

The main interest of this setup was the possibility to measure the aerodynamic effort for any angle of attack but the presence of the transversal support interferes with the flow and can introduce significant error.

Second configuration

The second configuration is similar to the first one but the balance and the driving mechanism are not in the wind tunnel but outside. The setup designed for the dynamic testing (see figure 8) was used for this purpose.

Last configuration

For the recent testing, the support is now a sting. The model for the static measurement is made in Ureol; a light material easy to machine. The reference length is 77mm in order to install the equipment inside (balances, encoder, oscillating mechanism). The balance was designed to fit into the model along the symmetry axis. The center of reduction of the balance is close to the center of mass for a better sensitivity (figure 5 and figure 6).

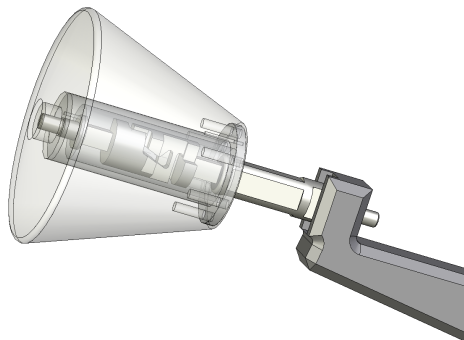


Figure 5: Model for the static tests with the balance

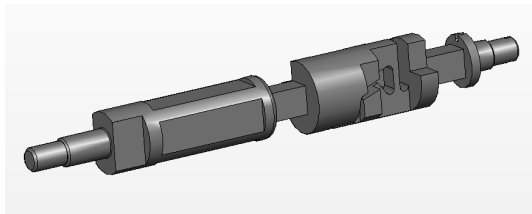


Figure 6: Balance for the static measurement

6.2.2. *Dynamic experiments*

Old configuration

The free to tumble setup used for the first campaign was developed during a previous study and modification was done in order to improve the quality of the angular measurement. The encoder is now able to give the angular position with 0.18° of accuracy. The picture (Figure 7) gives a general view of the set-up in the wind tunnel. The rod is mounted on two ball bearings and linked to the encoder in one side and to the release system on the other side. It is possible with this technique to know the exact angular position for an infinite range. When the center of gravity is not on the axis of symmetry, it is necessary to add a mass to equilibrate the model. Otherwise, the trim position is influenced by the actual position of the center of gravity and do not depend only of the aerodynamic characteristic. The model is made of foam and resin and the reference length is 50mm.

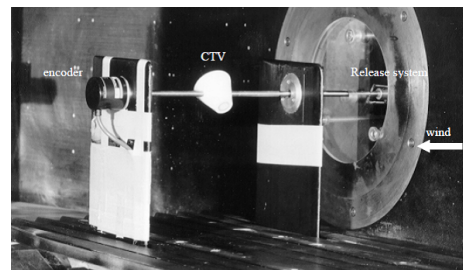


Figure 7: First Set-up for free to tumble test

Second configuration

A new setup was developed for the VKI S1 wind tunnel to support a model by a transversal rod. This rod is linked to a mechanism able to supply an oscillating movement or it is free to tumble. In this last case, an effort was made to limit the friction of the bearing to a minimum level. For this purpose, ceramic ball bearings were used because friction is very low when they are used without lubrication. A magnetic encoder will measure the angular position with high accuracy (4096 steps/revolution). In order to adjust the inertia of the model, a mass can be add on the support but the complete system must be as light as possible to reach the lowest value of inertia. For this purpose, particular care will be taken in the choice of material for the oscillating elements.

The previous experience shows problems in releasing system. It was not fast enough and it was difficult to adjust accurately the initial position. A new system was designed to allow fast and accurate

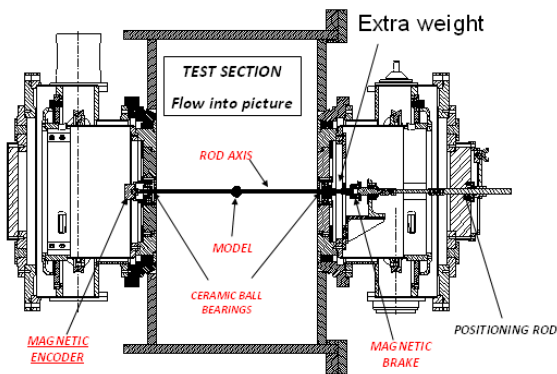


Figure 8: Experimental setup for free oscillations testing

angular release position. It is made of a small disk attached to the transversal rod and an electromagnet. This one can be operated by the operator thanks to a secondary axe passing through the wind tunnel.

New configuration

Like for the static efforts, when using a transversal support, the support disturbs the flow topology and produce significant error on the pitching moment measurement. The new setup was designed in order to produce the oscillations of the capsule through a sting. Since the aim of the study is to measure the forces applied on the capsule while oscillating. The setup is rather complicated (figure 9, 10 and 11):

- A big electrical motor is fixed outside the wind tunnel. It drives the model with the required frequency and amplitude.
- The rotation of the motor is transformed into oscillations thanks to an eccentric system.
- A secondary sting is then animated of periodic forward / backward translation movement inside of the main sting.
- The diameter of the main sting is selected to avoid excessive flexion during the tests campaign.
- Inside of the model, a static piece supports the encoder and the axis of the model.
- This axis is oscillating thanks to a crankshaft system and the balances are fixed on the axis.
- Interfaces between the balances and the model are adjusted together and should give a perfect trim position of the model.

- One optical encoder is fixed inside the model.
- For these dynamic measurements, the center of gravity is very important. It means that the center of rotation of the capsule should correspond to the center of gravity.

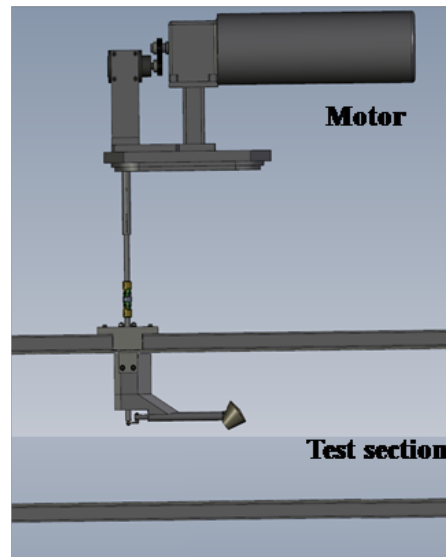


Figure 9: Overview of the dynamic set up

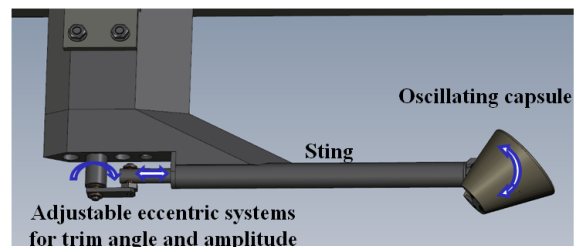


Figure 10: Zoom in on the oscillating system

The model is constructed in several parts which are then assembled on the balances which are fixed on the axis. The figure 11 gives a view of the different pieces composing the model.

To obtain the forces applied on the model during the experiments, an aerodynamic balance was designed (balance VKI3822). Two of them are placed inside the model for a better symmetry and so, a higher accuracy.

The four arms of the balance behave like four beams. The arm distortions are followed by the different distortion gauges stuck at different places on each arm. The center of reduction of the balance is located

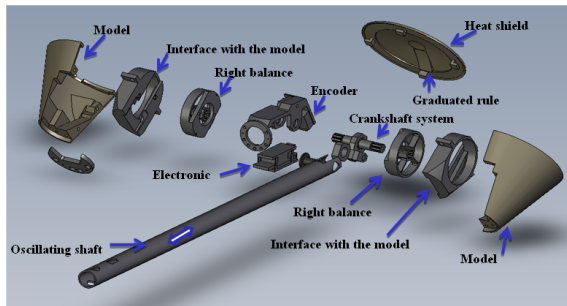


Figure 11: different pieces constituting the model

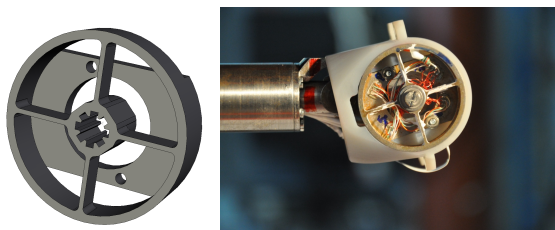


Figure 12: Dynamic balance

on the axis of rotation. The balance allows also the measurement of the axial and normal force in order to compensate for interferences.

7. Models manufacturing

As mentioned before, the model has to be light whatever the technique used. In case of free to tumble model, the model is light in order to respect the similitude and when the forced oscillation technique is used, the mass is reduced as much as possible in order to decrease the inertial part of the moment and increase the accuracy. Over the years, the technique used to build the model has changed. First models were built from foam and resin and the shape was obtained by casting. The problem of the casting was the accuracy of the shape of the model. Then, SLA prototyping was used because of the complexity of the model but this technique does not allow to control the shape of the model and the location of the CG. The last improvement consists in mixing the SLA for the complexity and the classical machining for the quality. It is the more precise way to build a model but improvements are still needed to decrease the uncertainty in CG location.

8. Results

Many results have been obtained over the years. This part gives typical results obtained with the CTV model.

8.1. Static tests

During the first campaign, the moment can be measured over a large range of angle of attack and the model is supported by a transversal rod. The results are given in the figure 13. The figure 14 shows the same measurement with the new setup. The range of angle of attack is limited to 15° . The slope is similar but the trim angle is very different ($\alpha \approx -40^\circ$ for the first campaign and $\alpha \approx -17^\circ$ for the second). These last measurements have been compared with literature data and good agreement is found (see figure 15). It clearly indicates the strong influence of the support for this kind of measurement.

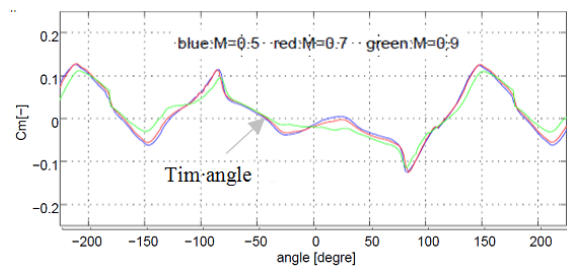


Figure 13: Pitching moment on CTV in transonic regime (first Setup)

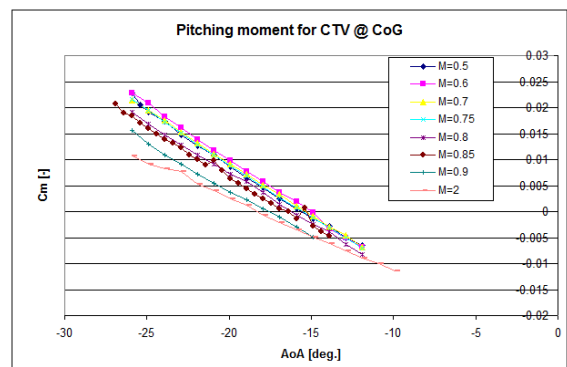


Figure 14: Pitching moment coefficient on the CTV capsule (new setup)

8.2. Dynamic tests

The dynamic test carried out during the first campaign consisted in qualitative measurement. The purpose of the tests was to measure the trim angle (figure

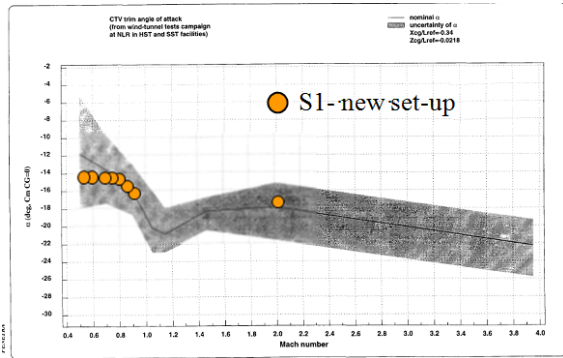


Figure 15: Trim angle of the CTV capsule (new set-up versus literature)

15) and to estimate the range of angle of attack for which the model is dynamically stable (see figure 16 and table 2). It can be noted that the dynamic trim angle is the same than the static one. The support was the same and produced the same effect. The phase diagram indicates clearly if the model is stable or not and it can be compared with static result. The trim points found by static experiments are confirmed with the dynamic setup and each of these points is stable.

model Mach # release angle	CTV Heavy		
	0.5 final angle	0.7 final angle	0.9 final angle
10	42.2 / 42.4	42.3 / 42.4	39.8 / 39.9
55	42.5 / 42.3 / 42.4	42.4	39.9
80	42.4	42.5	40.1
100	42.8 / 42.4 / 42.5	42.5 / -30.7	40.1 / 40.2
130	42.4 / 42.5 / LO / >>	42.6 / -30.7	40.2
155	42.4	42.5 / 42.4 / -30.7 / LO / >>	170.7
180	42.4 / LO / >>	171.4	40.3 / 40.4
200	42.4 / -34 / LO / >>	42.5 / -31.1 / LO / >>	40.3
225	>>	>>	>>
245	>>	>>	40 / 39.9 / LO / >>
270	43.6 / -34 / -33.8	42.5 / -31.1	40.2 / 38.9
310	42.3 / 42.4 / -33.8	42.5	40.1 / 40.2
330	-33.9 / -33.8	-31	40.3 / 40.2 / 39.6
0			

>> full rotation
LO : continuous Large Oscillation

Table 2: Final position of the CTV Capsule

The more recent dynamic experiments were performed with the forced oscillating mechanism supported by a sting. Experiments are carried out for various frequencies of oscillation in order to assess the sensitivity of this parameter. The damping parameter is computed using the energy method described before. For the CTV, the results are given in the figure 17. It shows the domain of similitude between 0.002 and 0.003. In this range, $C_{mq} + C_{m\dot{\alpha}} \approx$

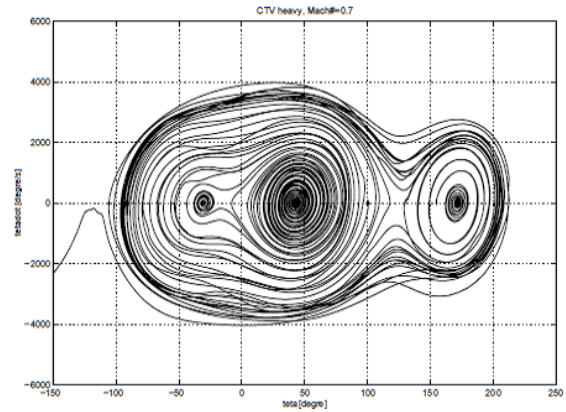


Figure 16: Phase diagram of the CTV capsule at Mach=0.7

+0.7. That means the vehicle is dynamically unstable. It is noted that for higher Strouhal number, the damping parameter is suddenly increasing. It happens for Strouhal =0.003 at Mach number of 0.9 and for Strouhal =0.006 at Mach number of 0.5.

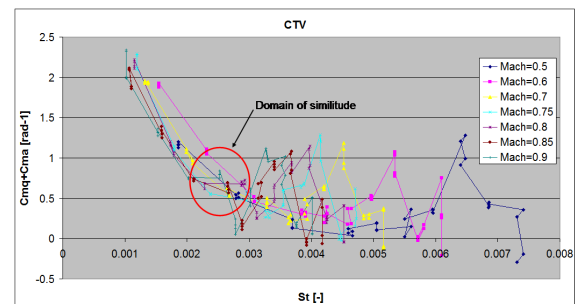


Figure 17: Damping parameter for the CTV capsule in subsonic regime

Dynamic results are given in the figure 18 for supersonic flow. For the CTV capsule, in the range of similitude, the damping parameter is clearly negative indicating stable behavior. A stable capsule in supersonic regime becoming unstable in subsonic is usual and not surprising. The phase diagram (only available for the subsonic regime) was showing opposite behavior, the vehicle was stable between Mach =0.5 and Mach=0.9

9. Error analysis

It is now clear that the transversal support introduced error. The recent experiment, carried out with a sting seems to give results of higher quality. Many aspect of the uncertainty have been studied. The error due to the balance is proportional to the one on

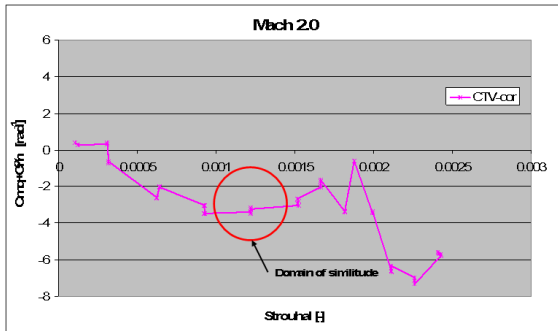


Figure 18: Damping parameter for the CTV capsule in supersonic regime

the damping coefficient (2.3%). The repeatability is good and the flow properties are very accurate. The more critical sources of uncertainty are coming from the CoG location, the balance stiffness, and the support effect. Many efforts have been done to respect the CoG and error is expected to be relatively small ($\text{err} < 0.1\text{mm}$). For the balance stiffness, a small shift in angle can happen between angle deduced from the rotation of the main driving shaft and the real angle. Under the maximum load of the balance, its flexure does not exceed 0.07° which corresponds to a shift on the main shaft of a bit less than 1° . The associated error on the damping parameter is deduced to be less than 35%. It is not possible to quantify the effect of the support because the reference value is not known.

10. Lesson learnt

During this project, models were designed and machined for static and dynamic experiments. In the last campaign, the static model was supported from the base through a balance. Due to the high sensitivity of the CoG location, very special care has to be taken to locate the center of reduction of the balance on the CG. An error of positioning of 0.1mm in the y direction produces a significant error on the trim angle. The model for the dynamic testing was much more complex as it must include the oscillating mechanism, two balances and the encoder. The fast prototyping technique allows producing light model with complex shape but results in not extremely accurate model. For this project, the outer shape of the model was further machined after assembly of all the elements with classical machining. At the end of this second step, some errors are still present in the positioning and it is suggested to investigate more on the way to produce the model for future campaign.

The forced oscillation mechanism allows adjusting the amplitude and the frequency of the model up to the required frequency to respect the similitude. The main difficulty came from gaps between pieces. The bronze bearing should be replaced by ball bearing or needle bearing in order to guarantee the movement with minimum friction and minimum gap for every couple of piece. The sting itself was big compared to the capsule. A significant part of the base of the model was removed to allow the passage of the sting. It is known that the sting introduces error in the force measurement but it should be minimized as much as possible. The design was made with such a big sting to avoid the flexion. Our experience from this campaign let us believe that the diameter can be further reduced.

The instrumentation for the static measurement is limited to the balance and the encoders used to measure the angle of attack. The balance should of course be correctly calibrated and special measurement must be taken in order to define precisely the location of the center of reduction. As explained before the definition of the trim angle of attack is very sensitive to the location of the center of reduction. For the dynamic experiment, two balances are used. The purpose of using two balances was to keep a good symmetry in the efforts, so that the interferences are limited. Possible improvements for the balance are the size and the stiffness. It is evident that the space in the capsule being limited, a smaller balance would help in the integration phase. Due to the strong oscillations during experiment and the gap between pieces, the balance must withstand high angular acceleration and deflection can be observed. A possibility is to increase the stiffness of the balance or to take it into account in the post-processing. The measurement of the angle of attack during the oscillating tests was initially expected to be measured by an encoder inside the model. It was finally decided to use an encoder outside the wind tunnel on the driving mechanism but the gaps between pieces introduced significant error and should be corrected by a correct modelisation of all the interfaces. If possible, the angle of attack should be measured as close as possible to the capsule in order to avoid multiple corrections.

The results for the static effort are in agreement with reference data for CTV. When compared to the measurement performed in the past at VKI with a transversal support, a large deviation is observed on the trim angle of attack. The transversal support is suspected to induce perturbation in the wake and to influence the measurement. Difference on the trim angle was about 20° . In the field of another ESA contract,

same kind of conclusion was done for the EXPERT vehicle. Both static and dynamic results are different depending on the support used (sting or transversal).

The CTV was already tested in the past with the transversal support and with the free to tumble technique. First of all, as already mentioned before, the trim angle was very different from the one obtained in the present campaign. Secondly, the dynamic behavior of the capsule was clearly stable over a large range of angle while it is now unstable. It is difficult to give a clear conclusion at that point about this difference. Possible source of error were discussed in the section 9. The support is one of the sources of uncertainty but the error cannot be assessed in the field of the present experiment.

The interference of the support on the flow has been shown by comparison between the present results and a previous campaign on CTV. This problem has also been demonstrated with the EXPERT vehicle by comparing the results from VKI and result from ITAM and SibNIA [17] on the same geometry but with a different supporting device. In both case the difference is significant for the static and dynamic testing. More investigation should be done to assess the support effect. As it is not possible to make experiment in wind tunnel without any support, it is proposed to investigate this effect with numerical tools. The first step consists in static computation in order to assess the effect of the supports and how they can affect the flow. In a second step, unsteady computation should be done on a static model. Comparison with existing experimental results should help in a better understanding the support effect and the topology of the flow. The final objective is to perform unsteady CFD on an oscillating capsule. Damping parameters can then be calculated with the same technique than the one used in wind tunnel.

11. Future work

Many results have been obtained with different experimental techniques. These results can be very different from one technique to another one and need to be properly validated. That will be the last part of this work. The purpose is to impose on the model a damping perfectly known when forced oscillations are applied. The method to deduce the damping parameter can then be used and results can be compared with the reference. Eddy current break was selected to impose a well-known damping. The advantage is to be able to vary the coefficient and eventually to impose a damping function of the angle of attack. This validation will give more confidence into the method

used to found the dynamic derivative. As explained before, the support plays an important role in the results. CFD tools will be used to assess the effect of the support. Better understanding of the flow around the model and the sting should help in choosing the best configuration to be used in wind tunnel to found the dynamic derivative.

12. References

- [1] S. Paris and J.M. Charbonnier, "Aerodynamic force and moment measurements and dynamic characterization of an Apollo capsule in the VKI S-1 wind tunnel", VKI, Internal note, 1997
- [2] O. Karatekin, "Aerodynamics of a planetary entry capsule at low speeds", VKI, PhD thesis, 2002
- [3] J. Yunis, "Analysis of forced oscillation, sting and tare force tests of subsonic and supersonic re-entry vehicles", VKI, Stagiaire report, 2007
- [4] E.S. Hanff, "Direct forced oscillation techniques for the determination of stability derivatives in wind tunnels", AGARD lecture series n°114 "Dynamic stability parameters", 1981
- [5] G.E. Burt and J.C. Uselton, "Effect of sting oscillations on the measurement of dynamic stability derivatives", Journal of aircraft, Vol.13 n°3, 1976
- [6] "Experimental determination of dynamic stability parameters", VKI, Lecture series 2008-02, 2008
- [7] R. Fail, "Experimental determination of stability and control aerodynamic characteristics", VKI, Lecture series 80 "Aircraft stability and control", 1975
- [8] D.M. Tang and E.H. Dowell, "Experimental investigation of three dimensional dynamic stall model oscillating in pitch", Journal of aircraft, Vol.32 n°5, 1995
- [9] S. Paris, J. Ouvrard and B. Torgler, "Free and forced oscillation testing of Apollo, Pares and Expert capsules", VKI, Contract report, 2008
- [10] D.I. Greenwell, "Frequency effects on dynamic stability obtained from small amplitude oscillatory testing", Journal of aircraft, Vol.35 n°5, 1998
- [11] F.Y. Wang, O. Karatekin and J.M. Charbonnier, "Low speed aerodynamics of a planetary entry capsule", Journal of spacecraft and rockets, Vol.36 n°5, 1999
- [12] E.S. Hanff and C.O. O'Leary, "Oscillatory test techniques", AGARD report n°776 "Special course on aircraft dynamics at high angles of attack: experiments and modelling", 1991

[13] L.E. Ericsson and J.P. Reding, "Review of support interference in dynamic tests", AIAA Journal, Vol.21 n°12, 1983

[14] K. Orlik-Rckemann, "Review of techniques for determination of dynamic stability parameters in wind tunnels", AGARD lecture series n°114 "Dynamic stability parameters", 1981

[15] B.L. Usselton and F.B. Cyran, "Sting interference effects as determined by measurements of dynamic stability derivatives, surface pressure, and base pressure for Mach numbers 2 through 8", AEDC-TR-79-89, 1980

[16] L.E. Ericsson, "Support interference", AGARD lecture series n°114 "Dynamic stability parameters", 1981

[17] S.Paris, A. Karitonov, J. Ouvrard SR 4000-VKI. Tool for the study of dynamic stability of reentry vehicle in the transonic/supersonic regime. Determination of aerodynamic damping coefficient of the Expert vehicle in transonic regime. Sept. 2010.